Scientific Research

Refined Numerical Simulation-Based Performance Analysis of Precast Segmental Prestressed Cap Beams

Hong Gan [1], Qing Zhang [1], Xingze Li [2] Yaohui Xue [2], Wei Cui [3,*] and Dinghao Yu [2]

[1] Jiangxi Ganyue Expressway Co., Ltd. Nanchang 330006, Jiangxi Province, China;
[2] Dalian University of Technology, Dalian 116024, Liaoning Province, China;
[3] Shanghai Municipal Prefabrication Technology Development Co., Ltd., Shanghai 200092, China.
* Correspondence: cuiwei5@smedi.com

Abstract: To address two critical challenges in the numerical modeling of precast segmental structures—namely, post-tensioned prestress simulation and adhesive joint representation—this study proposes a refined finite element modeling approach. This method incorporates a nearest point matching algorithm during prestress application, resolving issues such as modeling complexity and low computational efficiency in traditional tendon–concrete node matching. For adhesive joint simulation, a cohesive contact element based on fracture mechanics is adopted, enabling the characterization of tensile-shear coupled failure under combined loading conditions. To validate the method, a precast segmental prestressed cap beam from a real-world project was analyzed under prestressing and service load scenarios. The results demonstrate that the proposed approach is efficient, rational, and practically applicable, providing reliable technical support for high-fidelity numerical simulations of prefabricated structures.

Keywords: precast segmental structures; post-tensioned prestressing; adhesive joints; cap beams; cohesive contact elements

Citation: Gan, H..; Zhang, Q.; Li, X.; Xue, Y.; Cui, W.; Yu, D. Refined Numerical Simulation-Based Performance Analysis of Precast Segmental Prestressed Cap Beams. *Prestress Technology* **2025**, *3*, 38-51. https://doi.org/10.59238/j.pt.2025.03.003

Received: 23/06/2025
Accepted: 11/08/2025
Published: 30/08/2025

1 Introduction

Owing to their advantages of quality controllability, reduced environmental impact, and high standardization, precast segmental structural systems have been widely applied in bridge engineering and large-span spatial structures. In prefabricated concrete bridge structures, precast segmental prestressed beams feature rapid construction, strong adaptability to various service conditions, and suitability for a wide range of spans. They have been extensively used in the construction of key components such as box girders, piers, and composite beams. Based on numerous representative engineering projects worldwide, precast segmental prestressed beams are predominantly fabricated with transverse segmentation, and post-tensioning is often employed to take advantage of the flexible tendon arrangement to increase the load-bearing capacity. A series of studies [1–4] have demonstrated that joint type has a significant influence on the mechanical performance of precast segmental concrete beams, with adhesive joints providing remarkable performance compared with dry joints. Moreover, in practical engineering applications, various joint configurations are adopted, among which large shear keys, small shear keys, and corbel-type joints are commonly used.

In existing research, numerical simulation and experimental analysis are the two primary approaches for investigating the mechanical performance of structures or structural components. However, for precast segmental prestressed beams, performance analysis has thus far been dominated by experimental studies. Zhu Weidong et al. [5], using a 1:5 scale model test, examined the influence of different adhesive joint configurations on the mechanical behavior of large cantilever precast prestressed (PC) cap beams, highlighting the critical role of joint configuration. Based

https://doi.org/10.59238/j.pt.2025.03.003

on a 1:2 scale model, Li Lifeng et al. [6] investigated the diagonal cracking resistance and shear capacity of fully precast prestressed UHPC thin-walled cap beams. Zhuang Jianjie et al. [7] employed a full-scale test model to explore the damage and failure mechanisms of prefabricated piers under horizontal cyclic loading deeply. Gu Yin et al. [8] conducted a shaking table test to systematically study the dynamic response of prefabricated composite utility tunnels and identified structural weak points.

As an important complement to experimental studies, the application of numerical simulation methods in the field of segmental structures is still in the developmental stage. At present, mainstream numerical simulation approaches for precast prestressed members include the equivalent load method and the explicit tendon modeling method. In the equivalent load method, the commonly used implementations are the load method and the nodal force method, which are straightforward to apply: equivalent prestress loads are directly imposed on the concrete nodes. However, when the tendon profile is complex, the calculation of equivalent loads becomes difficult. Moreover, since prestressing tendons are not explicitly modeled, the stresses released following concrete cracking cannot be carried by the tendons, leading to divergence in the numerical results when the damage to the concrete becomes severe. The explicit tendon modeling method operates on a similar principle, with the initial strain method and the cooling method being the most common implementation. Both methods assign initial strain to the tendons during the prestressing stage so that prestress develops in subsequent analysis steps. Nevertheless, neither approach can efficiently reproduce the stress distribution in tendons after tensioning, and both consider tendon stress variations induced by structural deformation in a rather simplified manner [9–10].

Overall, refined modeling of precast prestressed members still faces numerous technical challenges. For precast segmental prestressed beams, post-tensioning with curved tendon profiles is typically employed to ensure favorable stress conditions. However, for tendons with complex three-dimensional geometries, accurate simulation of key parameters such as precise spatial positioning during stress and stress concentration effects induced by ducts remains difficult. Furthermore, modeling the complex non-linear behavior of adhesive joint interfaces under combined loading is challenging—particularly in capturing the asymmetry between tensile and compressive behavior and the intricate damage evolution process under tensile–shear coupling.

To address these challenges, this study proposes a refined finite element modeling method tailored for segmental structures, enabling both effective prestress application and rational simulation of adhesive joints. Based on the proposed approach, numerical analyses were conducted for a precast segmental prestressed cap beam under two loading scenarios—post-tensioned loading and concentrated loading—to validate the accuracy and applicability of the method. Finally, depending on the numerical results, optimization recommendations are proposed for prefabricated cap beam structures in terms of both cracking resistance and load-bearing capacity, providing a valuable reference for engineering design and construction.

2 Refined Numerical Modeling Method for Precast Segmental Prestressed Cap Beams

The overall modeling strategy for the precast segmental prestressed beam proposed in this study adopts a discrete (component-based) approach, in which each component—such as reinforcement, prestressing strands, and concrete—is modeled independently and then integrated through appropriate interaction definitions. Concrete is modeled using solid elements with the Concrete Damage Plasticity (CDP) constitutive model, which can accurately capture the stiffness degradation and

damage evolution of concrete under cyclic loading. Reinforcing bars and prestressing strands are modeled using linear beam elements with an ideal elastic–plastic constitutive law. To simulate post-tension in complex tendon configurations and novel adhesive joints, a nearest-point matching algorithm and a cohesive contact element method, respectively, are incorporated. Detailed descriptions of these techniques are provided in the following sections.

2.1 Post-Tensioned Prestress Application Based on the Nearest point Matching Algorithm

In segmental structural systems, the rational application of prestressing technology is a key factor in optimizing structural mechanical performance. Compared with the pretensioned state, the post-tensioned state offers greater flexibility in the tendon arrangement, better adaptability to long spans, and enhanced controllability of the prestress levels. Particularly when complex loading conditions, high durability requirements, and special construction constraints are addressed, posttensioning enables performance optimization through flexible stress control, thereby providing a reliable guarantee for engineering quality [11].

Currently, numerical modeling methods for post-tensioned prestressed concrete primarily fall into two categories: (1) both concrete and prestressing tendons are modeled with solid elements, where ducts are excavated within the concrete and cohesive elements are used to simulate prestress transfer; (2) concrete and prestressing tendons are modeled separately by solid elements and beam elements, respectively, while coincident nodal coordinates are maintained, and prestress transfer is simulated by establishing one-to-one connector elements or nonlinear spring elements between corresponding nodes [12–13].

Method (1) can realistically capture the contact behavior between prestressing tendons and concrete, as observed in actual engineering, but it greatly increases meshing complexity and often suffers from convergence difficulties. Method (2) generally results in good convergence but requires mesh compatibility between the concrete and tendon nodes. The traditional manual node matching approach is inefficient and lacks practical operability. This issue is particularly pronounced for curved tendon layouts, where irregular mesh patterns make accurate node correspondence difficult, resulting in a highly complex modeling process and hindering the accurate prediction of structural mechanical performance.

To address the node matching problem described above, this study proposes an efficient and accurate numerical simulation solution based on a nearest point matching algorithm (NPMA). The algorithm uses distance as a similarity metric between nodes and constructs a distance metric function to search in the feature space for the data object closest to the target object, thereby achieving high-precision matching. Given two sets of points in three-dimensional space, P and Q, the nearest-point matching algorithm iteratively searches for, according to the distance metric function defined in Equation (1), the point (x_2, y_2, z_2) in Q that has the minimum Euclidean distance to each point (x_1, y_1, z_1) in P, thus identifying the nearest point.

$$d = \sqrt{(x_1 - x_2)^2 + (y_1 - y_2)^2 + (z_1 - z_2)^2} \tag{1}$$

In the equation, the distance metric function is based on the Euclidean distance. Based on this principle, this study employs connector elements rapidly established via the nearest point matching algorithm to simulate the application of post-tensioned prestress. Compared with nonlinear spring elements, connector elements offer greater ease of use and extensibility (such as when duct friction is defined). As illustrated in Figure 1, the specific implementation procedure is as follows:

 https://doi.org/10.59238/j.pt.2025.03.003

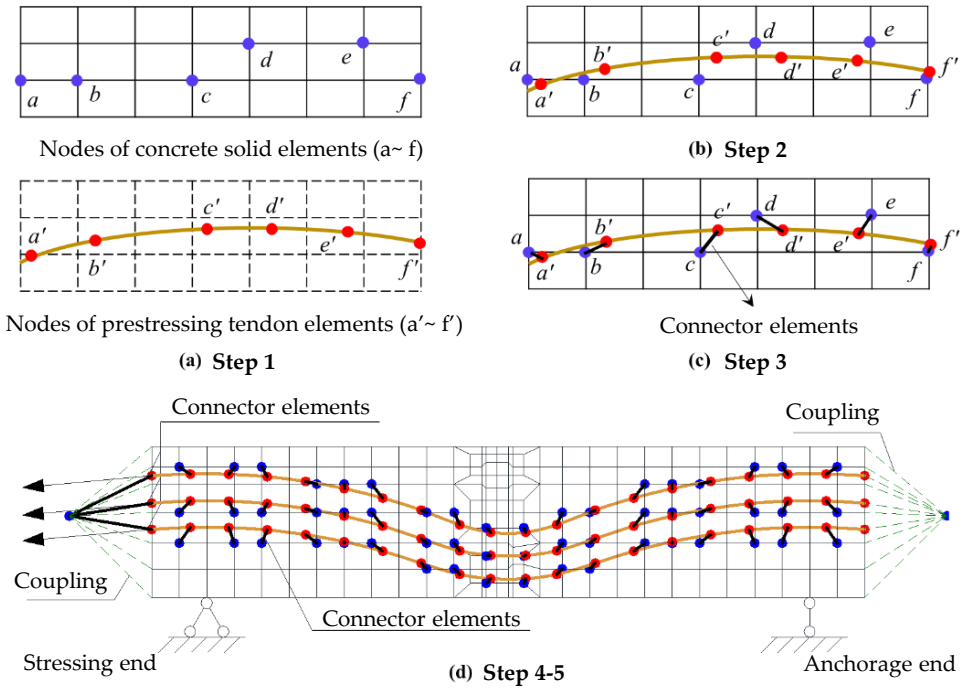

Figure 1 Illustration of post-tensioned prestress implementation based on the nearest-point matching algorithm

Step 1: Mesh Discretization

Finite element meshes are generated separately for both the concrete and the prestressing tendons.

Step 2: Automatic Node Matching

When the prestressing tendon mesh nodes are used as the primary node set, a spatial search algorithm automatically identifies the adjacent secondary node set within the concrete elements. Accurate node mapping is established based on the minimum Euclidean distance criterion.

Step 3: Connector Element Construction

Connector elements are established between each prestressing tendon node and the concrete node with minimum Euclidean distance. A local coordinate system is assigned to each connector, aligned with the cylindrical coordinate system at the center of curvature of the arcs forming the tendon profile. This ensures that the shear direction of the connector coincides with the geometric axis of the tendon. The connector element fully constrains the relative displacement in the normal direction, whereas a bond-slip constitutive model limits the relative slip in the shear direction. This configuration ensures that the forces from the concrete duct acting on the prestressing tendons during prestress application and subsequent loading are accurately transferred to the tendon nodes. Thereby precisely simulating their interaction.

Step 4: Prestressing Tendon Tensioning

To avoid stress concentration distortion in the concrete at the anchorage zone during simulation, a coupling constraint technique is employed. All the concrete surface nodes at the anchorage end are coupled together with the prestressing tendon end nodes to a common reference point. Similarly, all the concrete surface nodes at the stressing end are coupled to another common reference point, which is then connected to the prestressing tendon end nodes via connector elements. Prestressing tendon tensioning is achieved by shortening these connector elements. This approach effectively simulates the stress dispersion effect in the anchorage zone observed in practice and ensures uniform transfer of prestress from the anchorages to the

concrete structure, thereby enhancing the accuracy of finite element analysis. Furthermore, this treatment complies with the relevant provisions for local bearing pressure calculations in prestress anchorage zones, as specified in the "Specifications for Design of Highway Reinforced Concrete and Prestressed Concrete Bridges and Culverts" (JTG 3362—2018) [14].

Step 5: Boundary Condition Setup

The prestressing force at the end of Step 4 is maintained to simulate the anchorage effect. The support at the stress end is modeled as a fixed hinged support, constraining five degrees of freedom ($U_x, U_y, U_z, UR_y, UR_z$). The support at the anchorage end is modeled as a sliding hinged support, constraining four degrees of freedom (U_x, U_y, UR_y, UR_z).

Compared with traditional manual matching methods, the proposed approach establishes an accurate node mapping relationship that effectively mitigates numerical simulation distortions caused by non-uniform prestress distributions, ensuring high-precision control. Moreover, by incorporating three-dimensional spatial indexing techniques, the method significantly enhances the processing speed and computational efficiency for large-scale node matching. Notably, this approach demonstrates excellent applicability to practical engineering challenges such as complex three-dimensional tendon layouts, providing a reliable solution for the refined modeling of prestressed structures.

For convergence control of the nearest point matching algorithm, the distance tolerance based on the Euclidean metric is typically set below the average spacing between adjacent prestressing tendon nodes to avoid excessive redundant calculations during the three-dimensional spatial indexing process. Additionally, spatial partitioning techniques can be employed during algorithm implementation to perform neighborhood searches, whereby distance matching is conducted only within a specified range around the target linear element nodes, thereby improving computational efficiency.

2.2 Adhesive Joint Simulation Based on Cohesive Elements

The joint type plays a decisive role in the mechanical performance of segmental structures. Studies have shown that mechanical performance is significantly better for precast concrete beams connected by adhesive joints than for those connected by dry joints under equivalent conditions. Notably, their mechanical behavior in the elastic stage is essentially consistent with that of monolithically cast precast concrete beams [15]. Therefore, the refined simulation of adhesive joints is a key aspect of finite element model development. Existing studies typically model adhesive joints using tie constraints, solid cohesive elements, spring elements, or connector elements. However, tie constraints neglect fracture and stiffness degradation of the adhesive material, making it difficult to simulate interface debonding and damage accumulation. Although solid cohesive elements can capture the mechanical response of the adhesive layer, they require detailed solid modeling of the adhesive material, resulting in low modeling efficiency and high computational cost. Classical spring or connector elements can simulate the adhesive layer along individual axial or shear directions but lack fracture criteria that consider tensile–shear coupling effects, thus failing to accurately predict interface failure under combined loading conditions.

To address the issues, this study adopts a fracture mechanics–based cohesive contact element to simulate the mechanical behavior of the adhesive interface. This element incorporates damage criteria to represent the progressive failure process of the adhesive joint. The adhesive material is modeled using a bilinear constitutive law based on the Park–Paulino–Roesler (PPR) energy criterion, which defines tensile–

 https://doi.org/10.59238/j.pt.2025.03.003

shear coupled failure behavior through critical fracture energy and interface displacements. The uniaxial stress–displacement response is illustrated in Figure 2: During the elastic phase, stress increases linearly with displacement; in the softening phase, stress decreases linearly with damage accumulation to zero, dissipating all the energy. Here, σ and τ denote the normal and shear stresses, respectively; σ_0 and τ_0 are the normal and shear strength limits, respectively; δ_n and δ_s represent the normal and shear displacements, respectively; δ_{n0} and δ_{s0} are the initial damage displacements; and δ_{nf} and δ_{sf} are the failure displacements. This constitutive model assumes the elastic response of the adhesive interface under normal compression and considers failure only under tension and shear, which is consistent with the actual behavior of adhesive joints [16-17].

Notably, to avoid underestimation of the fracture energy caused by coarse meshing, local mesh refinement is applied at the midspan region of the beam based on the characteristic length theory. A simple transition mesh is used to balance computational efficiency and accuracy.

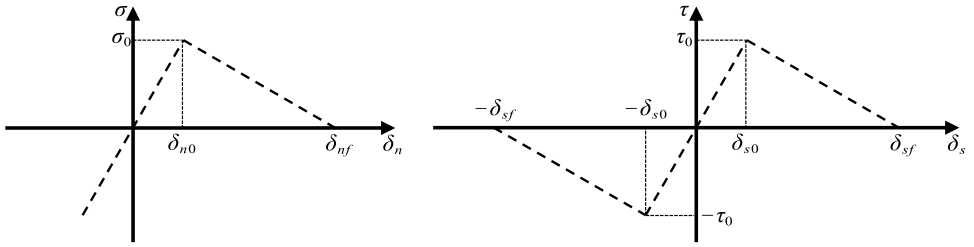

a) axial b) shear

Figure 2 Bilinear damage constitutive model of the cohesive contact element

3 Engineering Case Analysis

3.1 Overview

This study is based on the second phase of the Changzhang Expressway reconstruction and expansion project, in which a novel post-tensioned segmental precast cap beam is designed to accelerate construction and improve project quality. The member adopts an inverted T-shaped cross-section. The two precast beam segments are connected along the mid-span section through a combination of "corbel-type" joints and shear keys, with adhesive joints applied at the connection interfaces.

During construction, six curved grouted corrugated ducts are embedded prior to concrete casting. After the beam segments are fabricated and assembled on-site, high-strength prestressing strands are threaded through the ducts for post-tensioning, followed by anchoring, stressing, and end-sealing to complete the assembly.

The total design span of the cap beam is 18,329 mm, with an overall depth of 2,750 mm. The upper projecting portion is referred to as the top web, measuring 1,600 mm in thickness and 1,650 mm in height. The lower portion is the bottom flange, 3,400 mm wide and 1,100 mm in height. The prestressing tendons consist of high-strength steel strands (strand diameter 15.2 mm, cross-sectional area 180 mm²) symmetrically arranged on both sides inside the beam, following a curved profile and adopting reverse curvature near the tapered beam ends, as shown in Figure 3.

For the materials, C50 concrete is used for the beam segments. Longitudinal reinforcement consists of HRB400-grade reinforcement (diameters of 12 mm and 28 mm), whereas the stirrups are HRB400 reinforcement (diameter of 16 mm). The cross-sectional configurations at the mid-span and beam ends are shown in Figure 4.

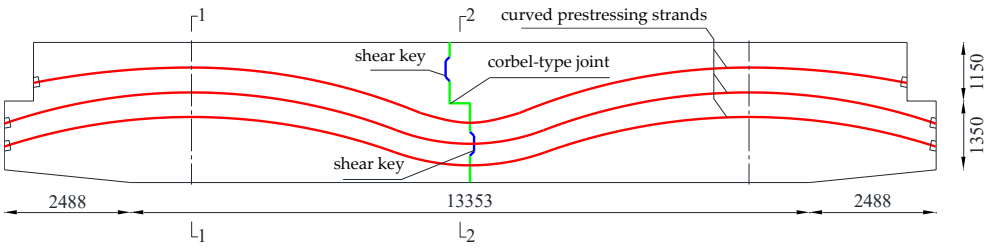

Figure 3 Half-section structural diagram of the prestressing strands in the cap beam

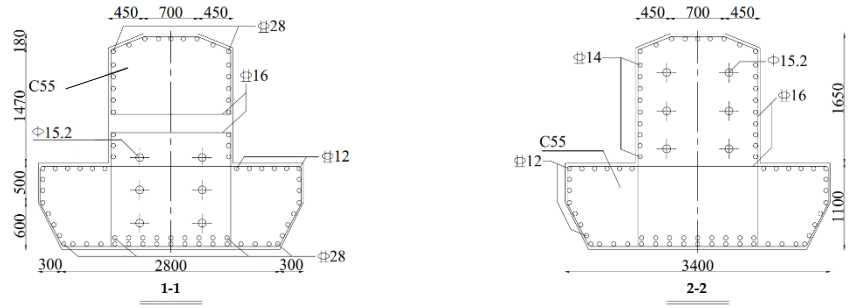

Figure 4 Cross-sectional details of the cap beam at the end (Section 1-1) and mid (Section 2-2) spans

3.2 Modeling

To investigate the flexure–shear coupled behavior of the precast cap beam, the sample shown in Figure 3 was selected as the research object. A refined numerical model was developed in ABAQUS, as illustrated in Figure 5. A partitioned modeling approach was adopted, where the concrete and bearing blocks were modeled using eight-node reduced integration solid elements (C3D8R). The reinforcement framework was simulated with two-node three-dimensional truss elements (T3D2), emphasizing their axial force characteristics. Prestressing strands were modeled with two-node spatial linear beam elements (B31), considering their stress state during prestress application and subsequent loading.

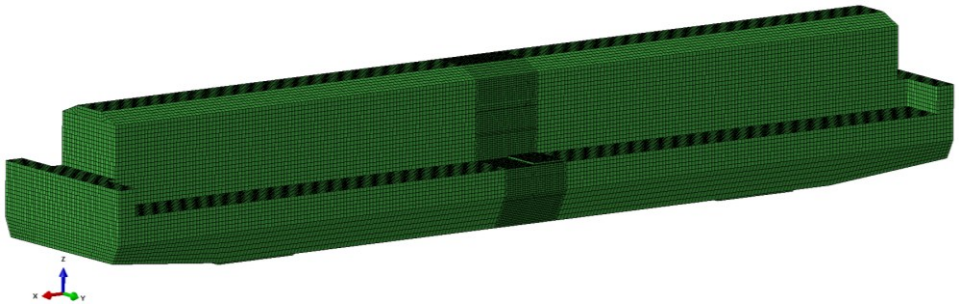

Figure 5 Finite element model

Concrete material behavior was characterized by using the Concrete Damage Plasticity (CDP) model, with the parameters listed in Table 1. The stress–strain relationships follow the uniaxial tensile and compressive constitutive laws prescribed by the "Code for design of concrete structures" (GB 50010—2010). Concrete tensile and compressive strengths were taken as standard values. The material yield strengths and elastic moduli of the reinforcement and prestressing strands are specified in Table 2.

To realistically simulate the interactions between components, appropriate contact conditions were applied. A tie constraint was used to fully bond the bearing

 https://doi.org/10.59238/j.pt.2025.03.003

blocks to the concrete beam, whereas an embedded region constraint ensured cooperative behavior between the reinforcement framework and the concrete. Epoxy resin mortar was adopted as the adhesive material for the joints; conservative material parameters were selected depending on the experimental results reported in [18–19] and are summarized in Table 3.

Table 1 Parameters of the concrete plastic damage model

Dilation angle ψ	Eccentricity e	Ultimate compressive strength ratio	Stress invariant ratio K_c	Viscous Parameter v
30	0.1	1.16	0.667	0.0005

Table 2 Material parameters of reinforcement and prestressing strands

Grade	Yield strength /MPa	Ultimate strength /MPa	Elastic modulus /GPa
Prestressing Strand ϕ^s15.2	1560	1860	195
HRB400Φ12	400	540	200
HRB400Φ16	400	540	200
HRB400Φ28	400	540	200

Table 3 Adhesive contact parameters of the epoxy resin mortar

Elastic modulus /GPa	Adhesive thickness /mm	Tensile strength /MPa	Fracture energy (J·m^{-2})
4.0	10.0	8.0	1200.0

The entire simulation was conducted using an explicit dynamic solver, which effectively handles complex contact and nonlinearities within the model, ensuring accuracy and reliability of the results. To minimize the influence of dynamic effects on outcomes, a sufficiently long loading duration was set to approximate static loading conditions. Furthermore, to enhance computational efficiency, a transitional mesh refinement was applied locally near the adhesive joint at mid-span. The refined concrete element size was controlled to approximately 40 mm within the densified region, whereas the coarse mesh elements outside this area were controlled to approximately 80 mm, thus reducing computational redundancy.

3.3 Response Analysis

3.3.1 Prestressing Strand Tension Analysis

To validate the rationality of the proposed modeling method, prestressing was applied to the beam, with the negative x-direction defined as the anchorage end and the positive x-direction as the stressing end. The displacement contours of the concrete beam segment after the application of prestressing are shown in Figure 6. The beam exhibited the expected camber during the stressing process, with the camber shape corresponding well to the geometry of the curved prestressing tendons. These findings preliminarily confirm the effectiveness of the proposed numerical modeling approach for post-tensioned prestressing.

The axial force distribution contours of the cross-sections of the prestressing strands are shown in Figure 7. The results indicate that the axial force in each strand gradually decreases from the stressing end to the anchorage end, which is consistent with the typical post-tensioning prestress distribution observed in actual engineering practice because of prestress losses, including friction losses, anchorage losses, and duct wall bearing effects [20].

The prestressing strand tension stress contours shown in Figure 8 reveal a relatively uniform stress distribution, with stress values concentrated between 1000

and 1290 MPa. This finding complies with the relevant provisions of Article 7.2.2 in the "Specifications for Design of Highway Reinforced Concrete and Prestressed Concrete Bridges and Culverts" (JTG 3362—2018), which stipulates the control stress for prestressing strands as $\sigma_{con} \leq 0.75 f_{ptk}$.

Furthermore, owing to the large curvature of the concrete duct at the beam mid-span, the duct wall typically induces stress concentrations in the prestressing strands. As depicted, the proposed modeling method effectively captures this local stress concentration phenomenon, further validating the modeling approach and ensuring the reliability of the subsequent load response analysis.

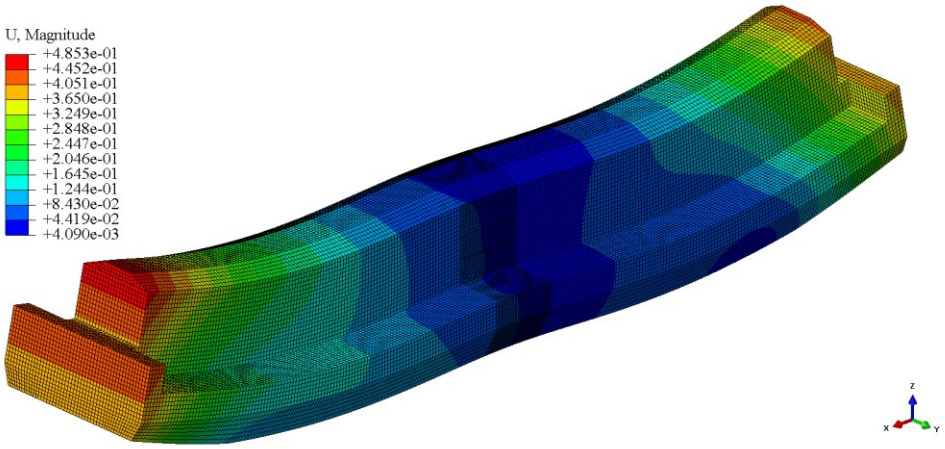

Figure 6 Concrete displacement contours of the beam segment

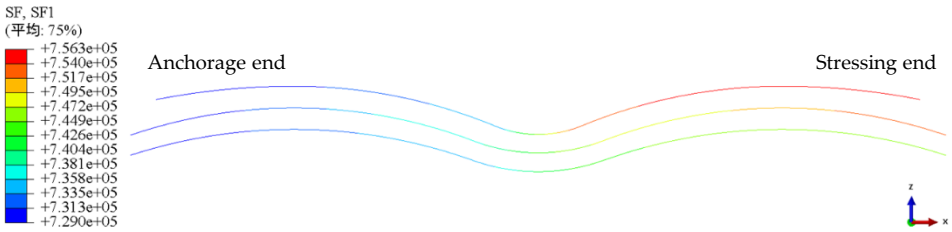

Figure 7 Axial force contours of the prestressing strands after tensioning

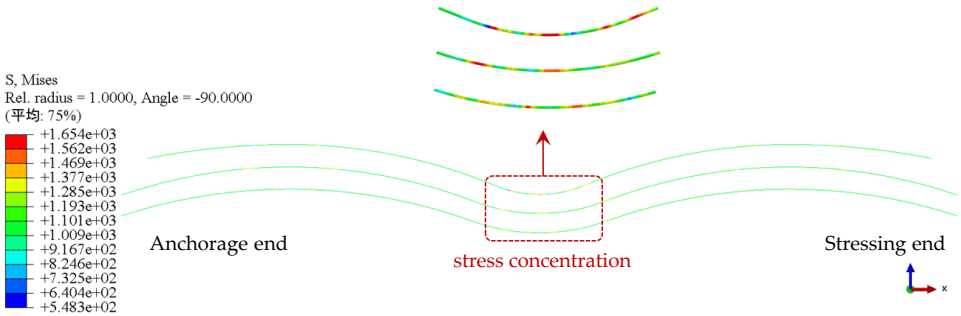

Figure 8 Stress contours of the prestressing strands after tensioning

3.3.2 Load Analysis

The adhesive joint region at the mid-span of the beam serves as a critical force transfer zone and is often the weakest part of the entire beam segment. To clarify the mechanical response characteristics of this region under loading, concentrated single-point forces were applied at the top of the flanges on both sides of the beam mid-span, as illustrated in Figure 9. The load–deflection curve at the mid-span was also calculated.

https://doi.org/10.59238/j.pt.2025.03.003

The deformation development and load-bearing behavior of the beam under applied loads can be divided into four main stages: the elastic stage (segment OA), the cracking stage (segment AB), the strengthening stage (segment BC), and the failure stage (segment CD), as shown in Figure 10.

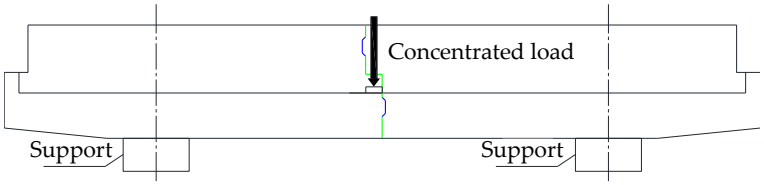

Figure 9 Schematic diagram of midspan loading

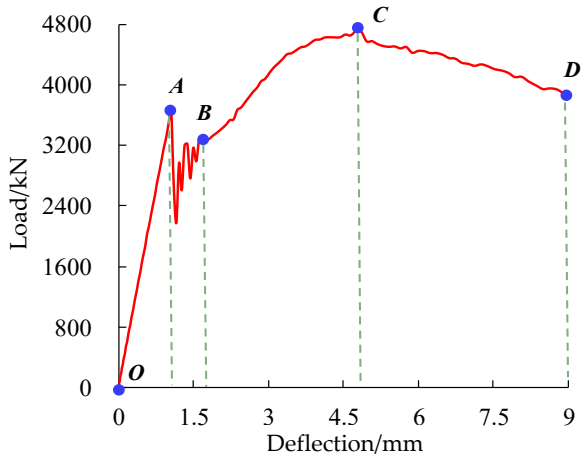

Figure 10 Mid-span load-deflection curve

Elastic stage (segment OA): The load–deflection curve is linear, with the concrete, reinforcement, and prestressing strands remaining in the elastic range. The beam demonstrates relatively high overall stiffness.

Cracking stage (segment AB): upon reaching point A, vertical cracks first appear at the bottom of the concrete near the mid-span adhesive joint, whereas progressive damage initiates from the root of the bottom shear keys in an upward direction. The damage contour of the beam segment at this stage is shown in Figure 11 a). As the load continues to increase, the plastic zone around the mid-span adhesive joint gradually expands, resulting in noticeable nonlinear fluctuations in the load–deflection curve.

Strengthening stage (segment BC): At point B, the internal force distribution within the section changes significantly: Compressive forces are primarily borne by the concrete at the top of the section and the adhesive material, whereas tensile forces at the bottom are almost entirely carried by the prestressing strands and ordinary reinforcement. At this stage, the bottom shear keys are nearly completely fractured, leading to a significant reduction in the shear capacity of the section. The damage contour of the beam segment is illustrated in Figure 11 b). As the load increases from point B to C, the beam clearly exhibits strengthening behavior: the tensile stress in the mid-span prestressing strands continues to rise, reaching a maximum tensile stress of 1604 MPa. Moreover, owing to deterioration in the collaborative performance between the strands and the concrete, damage occurs in the concrete duct progressively, causing further expansion of the plastic zone at the mid-span, which gradually extends toward the beam ends. This strengthening effect mainly arises from the strain hardening of the prestressing strands.

Failure stage (segment CD): When the load reaches point C, the prestressing strands at the mid-span approach yielding, and the beam reaches its ultimate load-bearing capacity. Moreover, significant damage accumulation occurs in the duct

region near the mid-span, as shown in Figure 11 c). During the loading process from points C to D, the damage zone at mid-span continues to expand until failure occurs. The damage condition of the beam segment at point D is illustrated in Figure 11 d).

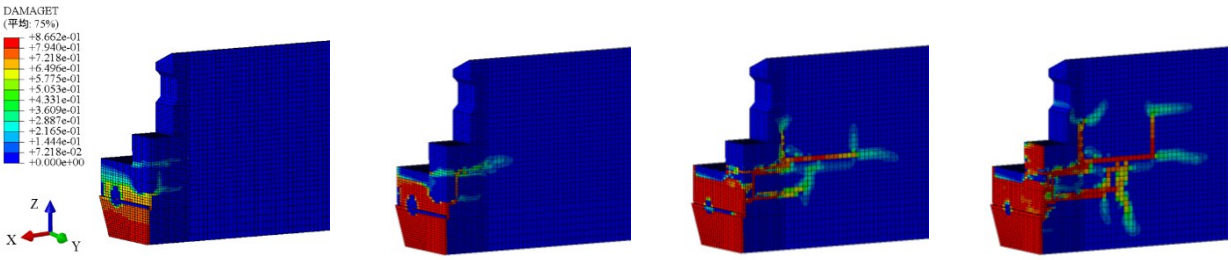

a) point A b) point B c) point C d) point D

Figure 11 Tensile damage contours of the beam segment

To investigate the influence of mesh sensitivity on the numerical simulation results, a comparative model with a mid-span mesh size of 80 mm was established for systematic analysis. The tensile damage contours of the beam segment at each stage are shown in Figure 12.

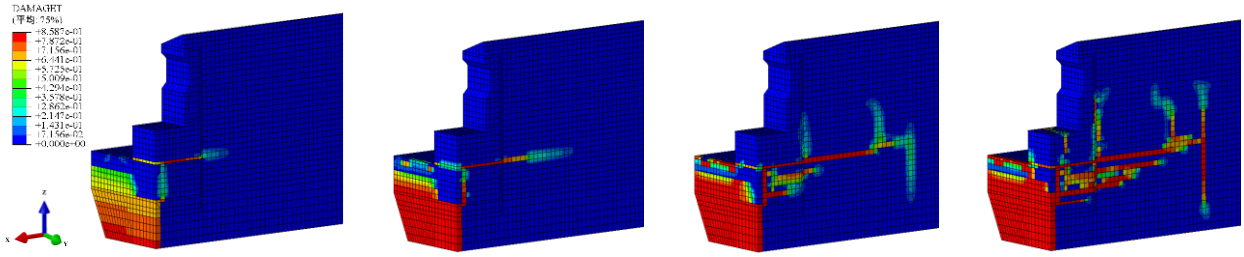

a) point A b) point B c) point C d) point D

Figure 12 Tensile damage contour plot of the beam segment with an 80 mm mesh size

The results indicate that although minor differences appear at certain stages between the 80 mm mesh model and the baseline 40 mm mesh model, both models exhibit a high degree of consistency in mechanical response throughout all stages. The initial crack locations and damage propagation patterns during the cracking stage, the internal force redistribution characteristics during the strengthening stage, and the ultimate failure behavior during the failure stage are in good agreement.

Notably, both mesh models accurately capture the fundamental features of the mid-span adhesive joint region as a critical weak zone, including preferential cracking of the bottom concrete, progressive damage to the shear keys, and the final failure mode controlled at the mid-span section.

Overall, the analysis suggests that stable numerical solutions can be achieved with mesh sizes of either 40 mm or 80 mm.

Furthermore, in accordance with the “Specifications for Design of Highway Reinforced Concrete and Prestressed Concrete Bridges and Culverts” (JTG 3362—2018), the ultimate flexural capacity of the beam’s mid-span cross-section is calculated to be 9931.1 kN·m. The finite element model predicts a value of 13,435.5 kN·m, yielding a ratio of the finite element result to the design value of 1.353. This observation indicates that the novel cap beam possesses a superior ultimate flexural capacity.

The above analysis indicates that the shear strength of the shear keys at the joints directly influences the crack resistance performance of the precast assembled cap beam, whereas the tensile strength of the prestressing tendons and the confinement effect provided by the ducts determine the beam’s ultimate load-bearing capacity.

https://doi.org/10.59238/j.pt.2025.03.003

Based on these findings, targeted measures can be adopted in engineering practice to optimize beam performance. For example, increasing the depth of shear keys or the effective shear area can enhance the design of shear keys in the mid-span adhesive joint region, thereby delaying the onset of initial cracks and improving the nonlinear response during the cracking stage. Utilizing higher strength prestressing strands and optimizing their spatial arrangement, along with improving the compaction of the concrete within the prestressing ducts, can enhance the bond performance between the strands and the concrete, reduce the stiffness degradation caused by interface slip, and increase the ultimate load capacity. Additionally, selecting low-shrinkage, high-strength modified epoxy adhesives and strictly controlling the aggregate size and mix proportion around the joints can improve the density and integrity of the adhesive interface.

4 Conclusions

This study addresses two key technical challenges in the numerical modeling of precast segmental prestressed beams: the application of post-tensioned prestress and the simulation of adhesive joints. By introducing the nearest point matching algorithms and the cohesive contact element method, a refined finite element modeling approach is proposed. Based on this method, a precast segmental prestressed cap beam from the second phase of the Changzhang Expressway expansion project was selected as engineering case for numerical simulation under prestressing and loading conditions. The following conclusions were drawn:

(1) The post-tensioned prestress application method based on the nearest point matching algorithm employed in this study automatically establishes an accurate mapping relationship between nodes of nonmatching meshes through spatial distance criteria. Compared with the solid tendon method, this method reduces model computational complexity by decreasing the number of elements and simplifies the contact relationship between the tendon and the concrete elements. Compared with node coupling methods, it achieves a breakthrough from monolithic modeling to component-based modeling and allows for separate definitions of bond-slip constitutive behavior in the tangential direction of the tendon and rigid constraints in the normal direction, thereby further improving numerical simulation accuracy. Prestress distribution simulated by this method aligns with practical engineering behavior, effectively capturing stress concentration effects caused by curved prestressing ducts and accurately representing the force process of post-tensioned prestressing strands overall. Given its tensioning process, the method is currently suitable for simulating post-tensioned prestress applications, whereas the simulation of pretensioned prestress applications require improvement.

(2) For precast segmental prestressed cap beams, the shear strength of shear keys at joints directly affects crack resistance performance, whereas the tensile strength of prestressing strands and the confinement effect of their ducts critically determine the ultimate load capacity of the beam. Based on this analysis, targeted measures can be proposed in engineering practice to optimize component performance.

Conflict of interest: All the authors disclosed no relevant relationships.

Data availability statement: The data that support the findings of this study are available from the corresponding author, Cui, upon reasonable request.

Funding: This research was funded by National Natural Science Foundation of China (grant number is 52378219) and Key Scientific Research Project of the Jiangxi Provincial Department of Transportation (grant number is 2025ZG012). The authors extended their sincere gratitude for the support.

References

1. Le, T.; Phan, T.; Hao, H.; Hao, Y. Flexural behaviour of precast segmental concrete beams internally prestressed with unbonded CFRP tendons under four-point loading. Engineering structures **2018**, *168(Aug.1)*, 371-383, doi: 10.1016/j.engstruct.2018.04.068
2. Le, T., Pham, T., Hao, H.; Yuan, C. Performance of precast segmental concrete beams posttensioned with carbon fiber-reinforced polymer (CFRP) tendons. *Composite structures* **2019**, *208(Jan.)*, 56-69, doi: 10.1016/j.compstruct.2018.10.015
3. Le, T.; Pham, T.; Hao, H.; Li, H. Behavior of Precast Segmental Concrete Beams Prestressed with External Steel and CFRP Tendons. *Journal of composites for construction* **2020**, *24(5)*, 04020053, doi: 10.1061/(ASCE)CC.1943-5614.0001059
4. Wrayosh, W.A.; Hashim, A.H. Flexural Behaviours of Box Segmental Beams with Internal Tendons Subjected to Repeated and Static Loads. In Proceedings of 3rd International Conference on Engineering Sciences (Part 2 of 3: Institute of Physics), Kerbala, Iraq, 4-6 November 2019.
5. Zhuo, W.; Li, C.; Sun, Z.; Xiao, Z.; Lin, Z.; Huang, X. Experiment on Static Behavior of Segmental Precast PC Cap Beam. *Journal of Tongji University (Natural Science)* **2022**, *50(12)*, 1752-1760.
6. Li, L.; Tang, J.; Hu, F.; Liao, R.; Ye, M.; Shao, X. Experimental on Shear Behavior of Prefabricated Light Weight Thin-walled UHPC Bent Cap. *China Journal of Highway and Transport* **2020**, *33(8)*, 144-158, doi: 10.19721/j.cnki.1001-7372.2020.08.015
7. Zhuang, J.; Li, C.; Jiang, H.; Lü, J.; Deng, L.; Xue, Z. Quasi-static experimental study on full-scale prefabricated bridge pier of Beijing-Xiong'an transit express line. *China Civil Engineering Journal* **2025**, *58(1)*, 90-100, doi: 10.15951/j.tmgcxb.23080705
8. Gu, Y.; Wang, H.; Lei, Z.; Yu, B.; Chen, M. Study on shaking table test of prefabricated assembly laminated pipe gallery. *Building Structure* **2025**, *55(10)*, 114-122+99, doi: 10.19701/j.jzjg.LS220239
9. Zhou, S.; Wang, J.; Leng, F. Prestress simulation and comparison for finite element analysis of concrete structure. *Yangtze River* **2015**, *46(24)*, 38-42, 47, doi: 10.16232/j.cnki.1001-4179.2015.24.010
10. He, L.; Wang, J. Method of Equivalent Load and Temperature Reduction on Prestressing Tendon for Effective Prestress Simulation. *Journal of Highway and Transportation Research and Development* **2015**, *32(11)*, 75-80.
11. Yang, H.; Guo, Z.; Xu, A.; Guan, D.; Feng, J. Experimental study on seismic behavior of local post-tensioned precast concrete beam-to-column connections. *Journal of Southeast University (Natural Science Edition)* **2019**, *49(6)*, 1101-1108.
12. Li, P.; Wang, J. Comparison of FEM Simulation Methods of Prestressed Reinforced Concrete Members. *Journal of Chongqing Jiaotong University (Natural Science Edition)* **2010**, *29(1)*, 27-29, 53.
13. Zhou, S.; Wang, J.; Leng, F. Prestress simulation and comparison for finite element analysis of concrete structure. *Yangtze River* **2015**, *46(24)*, 38-42, 47, doi: 10.16232/j.cnki.1001-4179.2015.24.010.
14. Zhao, T. Fem Analysis for Prestressed Anchorage System. Master's degree, Southwest Jiaotong University, Sichuan, China, **2003**.
15. Zhuo, W.; Li, C.; Sun, Z.; Xiao, Z.; Lin, Z.; Huang, X. Experiment on Static Behavior of Segmental Precast PC Cap Beam. *Journal of Tongji University (Natural Science)* **2022**, *50(12)*, 1752-1760.
16. Meng, D.; Huang, Y.; Lin, B. Study on The Bearing Capacity Performance of Steel Fiber Reinforced Concrete Structures Based on the Cohesive Zone Model. *Journal of Chongqing University* **2025**, *48(08)*, 54-66.
17. Yan, D.; Shi, Z.; Xu, Y. Analysis of Deformation and Damage in Ballastless Track-bed Based on Numerical Algorithm of Cohesive Zone Model. *Journal of the China Railway Society* **2024**, *46(9)*, 139-147.
18. Hang, Z.; Yu, Y. Experimental Research on Fracture Properties of Mixed Mode I-II Concrete-Epoxy Mortar Interface. *Industrial Construction* **2023**, *53(2)*, 29-36, doi: 10.13204/j.gyjzG22113007
19. Hu, X.; Wu, J.; Zhang, B. Fracture Simulation of Reinforced Concrete Beams Based on Cohesion Model. *Science Technology and Engineering* **2021**, *21(33)*, 14281-14286.
20. Zhang, Y.; Liu, S. Study of the loss of pre-stress of tendon in post-tensioned prestressed concrete beams. *China Journal of Highway and Transport* **2002**, *15(2)*, 76-78, doi: 10.19721/j.cnki.1001-7372.2002.02.019

AUTHOR BIOGRAPHIES

<table>
<tr>
<td>  </td>
<td>Hong Gan
B.E., Senior Engineer. Graduated from Xi'an Highway University in 1999 and working at Jiangxi Ganyue Expressway Co., Ltd.

Research Direction：Prestressed Bridge Structure.
Email: 756355392@qq.com</td>
<td>  </td>
<td>Qing Zhang
M.E., Senior Engineer. Graduated from Changsha Communications Institute in 1997 and working at Jiangxi Ganyue Expressway Co., Ltd.
Research Direction：Prestressed Bridge Structure.
Email: 411346069@qq.com</td>
</tr>
<tr>
<td>  </td>
<td>Xingze Li
M.E. (Candidate). Studying at Dalian University of Technology.
Research Direction：Prestressed Bridge Structure.

Email: 2845877528@qq.com</td>
<td>  </td>
<td>Yaohui Xue
D.E. Graduated from Daliang University of Technology in 2025.
Research Direction：Disaster Resistance of Large-Span Structures.
Email: xueyaohui1995@163.com</td>
</tr>
<tr>
<td>  </td>
<td>Wei Cui
B.E., Engineer. Graduated from Chang'an University in 2009 and working at Shanghai Municipal Prefabrication Technology Development Co., Ltd.
Research Direction：Concrete Bridges and Assembly of Industrialized Prefabricated Components.
Email: cuiwei5@smedi.com</td>
<td>  </td>
<td>Dinghao Yu
D.E., Senior Engineer. Graduated from Dalian University of Technology in 2019 and working at Dalian University of Technology.

Research Direction：Advanced Structural Analysis Method.

Email: ydh@dlut.edu.cn</td>
</tr>
</table>